

## Circulating Extracellular Vesicles Induce Monocyte Dysfunction and are Associated with Sepsis and High Mortality in Cirrhosis

Sukriti Baweja<sup>1</sup>, Chhagan Bihari<sup>3</sup>, Preeti Negi<sup>1</sup>, Swati Thangariyal<sup>1</sup>, Anupma Kumari<sup>1</sup>, Deepika Lal<sup>1</sup>, Deepanshu Maheshwari<sup>1</sup>, Jaswinder Singh Maras<sup>1</sup>, Nidhi Nautiyal<sup>1</sup>, Guresh Kumar<sup>1</sup>, Anupam Kumar<sup>1</sup>, Nirupama Trehanpati<sup>1</sup>, Gautam Mehta<sup>4,5</sup>, Ashok Kumar Chaudhary<sup>2</sup>, Rakhi Maiwall<sup>2</sup>, Shiv Kumar Sarin<sup>1,2</sup>

<sup>1</sup>Department of Molecular and Cellular Medicine, Institute of Liver and Biliary Sciences, New Delhi, India

<sup>2</sup>Department of Hepatology, Institute of Liver and Biliary Sciences, New Delhi, India.

<sup>3</sup>Department of Pathology, Institute of Liver and Biliary Sciences, New Delhi, India.

<sup>4</sup>Institute for Liver and Digestive Health, University College London, UK.

<sup>5</sup>Institute of Hepatology, Foundation for Liver Research, London, UK.

**Short Running Title:** Role of Extracellular Vesicles in Cirrhosis and Sepsis

**Word Count of manuscript:** 4833

**Disclosure:** All authors have declared no conflict of interest.

**Patient consent** - Obtained.

**Ethics approval** - Institutional Ethics Committee, Institute of Liver and Biliary Sciences, New Delhi, India.

Reference number is F.25/5/81/ILBS/AC/2015/910.

**Financial Support:** This work is funded by institutional research support grant.

**Author's Contribution:** SB and SKS designed the study protocol and the overall supervision. SB, CB, PN, ST, DL, NN, A Kumari, DM performed the experiments, data collection and analysis. JSM, GK contributed for the statistical analysis. NTP, AK, GM, ASC gave the material support and sample collection. RM and SKS gave the intellectual support and proof reading. All the authors have approved this manuscript.

**Abbreviations:** EV; Extracellular vesicles, Child; Child-Turcotte-Pugh, TLC; Total leucocyte count, AST; Aspartate amino transferase, ALT; Alanine aminotransferase, PT; Prothrombin time, INR; International normalized ratio, HC; Healthy Control, BM; Bone Marrow, HSC; hematopoietic stem cells, M $\phi$ ; Macrophage,

This article has been accepted for publication and undergone full peer review but has not been through the copyediting, typesetting, pagination and proofreading process, which may lead to differences between this version and the [Version of Record](#). Please cite this article as [doi: 10.1111/liv.14875](https://doi.org/10.1111/liv.14875)

This article is protected by copyright. All rights reserved

ASGPR; Asialoglycoprotein receptor, Tc; Cytotoxic T cells, Th; T helper cells, OCR; oxygen consumption rate, ETC; electron transport chain, IL; interleukin, MCP1; monocyte chemoattractant protein1.

**Correspondence:** Dr S K Sarin, MD, DM, D.Sc. (Hony.)

Senior Professor, Department of Hepatology,

Institute of Liver and Biliary Sciences, New Delhi, India

shivsarin@gmail.com, sksarin@ilbs.in Tel: 011-46300000, Fax 011-26123504

## Abstract:

**Background:** Sepsis is common in cirrhosis and is often a result of immune dysregulation. Specific stimuli and pathways of inter-cellular communications between immune cells in cirrhosis and sepsis are incompletely understood. Immune cell-derived Extracellular Vesicles (EV) were studied to understand mechanisms of sepsis in cirrhosis.

**Methods:** Immune-cell derived EV were measured in cirrhosis patients [Child-Turcotte-Pugh (Child) score A, n=15; B n=16; C n=43 and Child-C with sepsis (n=38)], and healthy controls (HC, n=11). *In-vitro* and *in-vivo* functional relevance of EV in cirrhosis and associated sepsis was investigated.

**Results:** Monocyte, neutrophil and hematopoietic stem cells associated EV progressively increased with higher Child score ( $p<0.001$ ) and correlated with liver disease severity indices ( $r^2>0.3$ ,  $p<0.001$ ), which further increased in Child C sepsis than without sepsis ( $p<0.001$ ); monocyte EV showing the highest association with disease stage [ $p=0.013$ ; Odds ratio-4.14(1.34-12.42)]. A threshold level of monocyte EV of 53/ $\mu$ l predicted mortality in patients of Child C with sepsis [Odds ratio-6.2 (2.4-15.9), AUROC=0.76,  $p<0.01$ ]. *In vitro* EV from cirrhotic with sepsis compared without sepsis, induced mobilization arrest in healthy monocytes within 4 hours ( $p=0.004$ ), reduced basal oxygen consumption rate ( $p<0.001$ ) and induced pro-inflammatory genes ( $p<0.05$ ). The septic-EV on adoptive transfer to C57/BL6J mice, induced sepsis like condition within 24h with leukocytopenia ( $p=0.005$ ), intrahepatic inflammation with increased CD11b+ cells ( $p=0.03$ ) and bone marrow hyperplasia ( $p<0.01$ ).

**Conclusion:** Extracellular vesicles induce functional impairment in circulating monocytes and contribute to the development and perpetuation of sepsis. High levels of monocyte EV correlate with mortality and can help early stratification of sicker patients.

**Keywords:** Immune cell-associated extracellular vesicles, Liver cirrhosis, Sepsis, Systemic Circulation, and Cirrhosis associated immune dysfunction, infections in cirrhosis.

## Lay Summary

Serious infection (sepsis) in patients with cirrhosis is frequently associated with immune cell defects. Extracellular vesicles (EV) carry different types of information depending on the type of injured cell, and in turn, can affect the function of other cells including immune cells. Here, we have identified monocyte

associated EV increase progressively with increase in severity of cirrhosis, and can predict risk of death. Also, EV from cirrhosis patients with sepsis can induce functional defects in healthy monocytes. Additionally, if EV from septic mice are transferred into healthy mice, a sepsis-like condition can be developed. Study of EV gives us an opportunity to identify them as potential sepsis biomarkers and pave way to develop EV based therapeutic strategies.

#### **INTRODUCTION:**

Cirrhosis represents the end-stage of many liver diseases and afflicts millions of people worldwide. Liver transplantation remains the only curative therapy (1). Cirrhosis is associated with ongoing fibro-inflammatory injury, concomitant systemic inflammation and immune defects, which collectively have been termed cirrhosis-associated immune dysfunction (CAID)(2) (3). Superimposed infection on the background of cirrhosis is a common cause of deterioration in cirrhosis, leading to rapid decline of liver function, sepsis and multi-organ failure, with mortality rates of up to 70% (4). The pathobiology of CAID is only partly understood, although is likely to be due to constant low grade immune stimulation and gradual exhaustion of innate and adaptive immunity. Potential mechanisms include 'exhaustion' of immune cells due to continuous exposure to damage-associated molecular patterns (DAMPs) or pathogen associated molecular patterns (PAMPs) which lead to continuous immune cell stress or cell death(5) . However, the specific stimuli of CAID and pathways of inter-cellular communication between immune cells in cirrhosis have not been identified so far.

Extracellular vesicles (EV) are small and heterogeneous membrane-bound structures released by cells under normal physiological conditions, and their level increases as result of cellular stress. EV are found in all biological fluids and are effective inter-cellular communicators. EV can transport a variety of bioactive molecules, including messenger RNA, noncoding RNAs, proteins, lipids, and metabolites between cells and can regulate various cellular responses (6) (7). Additionally, EV cargo may reflect the cell of origin as well as the specific stress that induced their formation and release (8). Alterations in the concentration and

composition of EV in biological fluids may reflect the status of different pathologies in liver diseases (9). We have recently demonstrated that EV associated with hepatocytes and hematopoietic stem cells can serve as early predictors of response to corticosteroid therapy in severe alcoholic hepatitis (SAH). In this study, the concentration of EV was found to be associated with severity of the liver disease, and from SAH patients induced pro-inflammatory cytokine production in healthy monocytes and neutrophils (10). These observations led us to focus on the role of EV in cirrhosis and associated sepsis. Prior work has demonstrated that a key event in the progression of liver cirrhosis is a dysfunctional immune response arising from exacerbation of systemic inflammation and immune cell paralysis (11). The current study is focused on EV associated with immune cells. Several studies indicate that EV can affect cellular functions, and released EV do not only stay in the tissue of origin, but also circulate in the blood to facilitate inter-cellular communication (12). High-grade systemic inflammation due to activation and dysregulation of the monocytes leads to release of danger signals and causes immune cell death (13). However, the specific mechanisms of immune cell failure in cirrhosis, and predisposition to sepsis, remain only partially described.

The hypothesis of this study was that circulating EV in cirrhosis are causally associated with immune cell dysfunction. The specific aim of the present study was to obtain a comprehensive view of the landscape of immune cell-derived EV in cirrhosis, with or without sepsis. Further, to understand the functional significance of EV in monocyte regulation and development of sepsis, we investigated EV-monocyte crosstalk *in vitro*, in cirrhosis with or without sepsis. Finally, we investigated the potential of EV from a mouse model of sepsis to transfer a sepsis-like phenotype *in vivo*.

## **PATIENTS AND METHODS:**

### **Patients Selection and Sample Size:**

*Inclusion Criteria:* A total of 74 patients with alcohol associated liver cirrhosis were enrolled. The inclusion criteria were; age between 18 and 65 years, compensated, decompensated cirrhosis [based on clinical, imaging, endoscopic, with and without histology]. Both out and in patients were included. Patients with different severity of cirrhosis as per Child-Turcotte-Pugh (Child)stage [Child A, n=15; B, n=16; C, n=43] were enrolled. Patients with Child C and sepsis n=38 were all in-patients, while patients without sepsis were

enrolled from out-patient. Majority of patients of sepsis had history of prior decompensation (Jaundice, ascites, hepatic encephalopathy or variceal bleed).

Sepsis was defined as described (14) briefly, organ dysfunction due to microbiological infection.

We also included a group of age and sex matched healthy subjects, who had no previous or present history or evidence of any liver ailment as controls (n=11). Institutional review board approved the protocol [reference no. F.25/5/81/ILBS/AC/2015/910] and patients were enrolled after taking informed written consent.

*Exclusion Criteria:* The patients with recent blood or blood component transfusion in the last 2 weeks; positive serology for human immunodeficiency virus infection; hepatitis viruses, antiplatelet, anticoagulant, or antifibrinolytic therapy; dialysis; pregnancy; active malignancy in the last 5 years; patients with HCC, chronic heart failure; and/or chronic pulmonary or end-stage renal disease, patients on immunosuppressants, post liver transplants, were excluded.

This was a prospective cohort study and the samples were collected at the time of enrolment and all the relevant clinical details were recorded. The data was correlated with mortality. Patients were managed according to the standard of care. Antibiotics were administered to the patients with infections in accordance with institutional guidelines.

**Blood Collection:** Twenty microliter of whole blood was collected from patients or healthy volunteers. Subsequently, the sample was subjected to RBC lysis followed by immune-phenotyping by flow cytometry (see below). Peripheral blood mononuclear cells (PBMCs) were isolated using ficoll hypaque (Himedia, USA) and an adherent method was used to separate monocytes by incubation for 2h in CO<sub>2</sub> incubator in RPMI complete media with 10% FBS. Plasma was separated and stored at -80° C until used further for EV isolation and studies.

**Sample Processing:** Guidelines by International Society on Thrombosis and Haemostasis (ISTH) were followed for extracellular vesicles. Samples were processed within 2h of collection. The tubes received no agitation, aside from a single inversion of the tube just prior to first centrifugation. Special attention was given to sample collection, time delay before first centrifugation, agitation, storage and thawing.

**Isolation Of Circulating Extracellular Vesicles By Differential Ultracentrifugation:**

Circulating EVs were isolated using differential centrifugation and ultracentrifugation. Two initial centrifugation steps at 10,000 rpm were performed to remove platelets and debris. Subsequently, careful centrifugation was performed at 100,000g for 30 minutes to pellet the EVs. An extra washing step was also performed at 100,000g with 1x PBS, to further remove any debris. The collected pellet was then enumerated by Nanoparticle tracking assay using Nano sight NS300 and flow cytometry to confirm extracellular vesicle populations as detailed previously (9).

#### **Characterization Of Circulating Extracellular Vesicles And Enumeration Using Multi-colour Flow Cytometry:**

EVs were enumerated using flow cytometry. Briefly, the isolated EV pellet was resuspended in 440µL of Annexin V binding buffer (diluted 1:10 in distilled water). All buffers were sterile-filtered with 0.2µm filter (Whatman). The samples were incubated for 15 minutes in the dark at room temperature, then diluted in 200µL of Annexin V binding buffer and immediately analysed on BD FACS verse (BD Biosciences, San Jose, CA). Spherotech latex beads (IL, USA), at four different sizes (0.22µm, 0.44µm, 0.88µm, and 1.0µm), were used to confirm the size of EVs. Forward-scatter and side-scatter had a logarithmic gain. The absolute count of EV was measured setting the stop condition for Trucount beads at 10,000 events. In order to separate true events from background noise and non-specific binding of antibodies to debris, we defined EV as particles that were less than 1.0µm in diameter, stained positively for Annexin V, and expressed surface antigens, as the threshold of the cytometer was set on Annexin V+ only. The data was analysed using Flow Jo software (Tree Star Inc., Ashland, OR). The absolute count of EV/µl was determined using the following calculation.

$$\text{Absolute cell count/}\mu\text{l} = \frac{\text{Cell count obtained}}{\text{Bead count obtained}} \times \frac{\text{Total bead count}}{\text{Total volume of sample}}$$

**Immune-phenotyping:** Whole blood was collected in EDTA vials and lysed by RBC lysis. It was washed twice with 1x PBS and followed by staining with fluorochrome labelled monoclonal antibodies for neutrophils (CD11b+ CD16+), classical monocytes (CD14+ CD16-; BD Biosciences, USA), dendritic Cells (lin- CD11c+, CD11b+; Bio legend, USA ), T cell subtypes ( CD3+CD4+;BD Biosciences, USA), (CD3+ CD8+ ;BD Biosciences, USA), B cells (CD3- CD19+ BD Biosciences, USA, Bio legend, USA ) HSC (CD45+CD34+ Bio legend, USA). The cells were acquired on BD FACS verse flow cytometer and were analysed using Flow Jo software (BD Biosciences, USA). The gating strategy is provided as Supplementary Figure 4.

**Co-culture of EV with Monocytes:** Monocytes ( $1 \times 10^5$ ) were isolated from healthy human volunteers using differential gradient ficoll hypaque method. These cells were then co-cultured with isolated EV (counted using flow cytometry and liquid counting beads (BD Biosciences, USA) from Child C patients without sepsis, Child C patients with sepsis, and healthy subjects (Cells: MV, 1:100) for 24h in RPMI media with 0.1% FBS and glutamine, as published previously (9). After 24h, the cells were harvested for studying monocyte functional changes post EV co-culture for further investigations as below:

*Uptake assay of EV:* Using 1ul of PKh67 dye,  $1 \times 10^8$  EVs from healthy, Child-C with sepsis and Child-C without sepsis were labelled and incubated with ( $1 \times 10^5$ ) cells healthy monocytes and the fluorescence was analysed at wavelength 568, using EVOS microscope (Thermo-Fisher Scientific, USA).

*Trans-well assay of monocytes:* Using the trans-well chamber, the migration of monocytes in presence or absence of EVs was evaluated. Healthy monocytes in suspension were loaded on top and EVs were added from Child-C with sepsis and Child-C without sepsis, and after 2h, 4h, 6h and 12h the cells were counted in lower chamber. MCP-1 was used as positive control and EV-depleted supernatant as negative control to evaluate the migration of healthy monocytes.

*Bioenergetics of monocytes using seahorse:* The Agilent Seahorse XF platform was used to measure the mitochondrial-stress test, which is the key parameter of mitochondrial function, by directly measuring the oxygen consumption rate (OCR) of cells. Sequential compound injections were given to measure basal respiration, ATP production, proton leak, maximal respiration, spare respiratory capacity, and non-mitochondrial respiration. The Seahorse XF Cell Mito Stress Test kit was used as per the manufacturer's protocol - oligomycin, FCCP, and a mix of rotenone and antimycin A were serially injected to measure ATP production, maximal respiration, and non-mitochondrial respiration, respectively. Proton leak and spare respiratory capacity were then calculated using these parameters and basal respiration.

*Quantitative real time PCR:* Total RNA was isolated from monocytes using ambion RNA Isolation kit according to the manufacturer's instructions. cDNA was prepared using high capacity cDNA reverse transcription kit (AB4368814, Applied Bio systems, Foster City, CA). Gene expression analysis using RT-PCR was performed by using applied bio-systems syber green assay kit (AB4309155) in Real-Time PCR System (ABI Vii7). Selected

candidate genes were investigated from inflammatory pathways such as caspase 1, 3 and 9; B cell lymphoma 2 (Bcl2); Bcl2 associated X (BAX); toll like receptors (TLR) 2, 4; Nod-like receptor proteins (NLRP) 1 and 3; Interleukins (IL)1b, 33 and 18; chemokine receptor (CCR) 3 and CXCR1, intercellular adhesion molecule 1 and 3, along with 18s as an endogenous internal control in monocytes. The data was represented in fold change keeping healthy control gene expression as reference control.

*Cytokine profiling:* After 24h of incubation, in the supernatants of the cultures was used for estimating IL-1b, TNF-a and IL-10 measured using a sandwich ELISA according to manufacturer's protocol (Elabsciences, China). The chromogenic detection was done at wavelength of 405nm/459nm/545nm respectively. The values were expressed in pg/ml. The lowest detection limit for IL-10 was 7.5pg/ml and for IL-1b and TNF-a was 15pg/ml.

*Phagocytosis Assay of Monocytes:* Phagocytosis in monocytes were performed using a commercial ex -vivo phagocytosis assay kit (IgG FITC), phago-test kit (Orpagen Pharma, Heidelberg Germany; cat no. 500290). Briefly, 100uL whole blood from healthy volunteers was collected in EDTA and incubated with 5 µL of FITC-labelled opsonized Escherichia coli(23107) and incubated at 37°C in a water bath for 40 minutes, washed with ice cold phagocytosis buffer. The cells were labelled with fluorochrome anti-CD14 antibody and acquired on BD biosciences FACS verse and analysed using FCS express.

**Animal Studies:** This animal study was approved by the Institutional Animal Ethics Committee of the Institute of Liver and Biliary Sciences (IAEC/ILBS/17/01 and IAEC/ILBS/17/02). C57BL/6 mice were procured from the in-house breeding of centre of comparative medicine, Institute of Liver and Biliary Sciences, New Delhi, India. All the animals received humane care according to the criteria outlined in the "Guide for the Care and Use of Laboratory Animals" Eighth Edition (2011) published by National Research Council of the National Academics, and Committee for the purpose of control and supervision of experiments on animal (CPCSEA) guidelines. C57BL/6 , Male mice age 8–9 weeks were injected with 50% carbon tetrachloride (CCl4) (0.5mg/ml/kg body weight) intraperitoneally thrice a week for 10 weeks for *cirrhosis model*. For the *sepsis model*, Caecal Ligation puncture (CLP) procedure was performed according to Dejager L et.al 2011. 10-12 weeks male mice briefly anaesthetized under isoflurane anaesthesia 1cm incision was made in the abdominal and caecal was exposed, ligated with 3/0 silk suture in the middle and puncture was performed with 21G

needle The abdominal musculature and skin were closed separately with 5/0 silk suture in simple continuous and interrupted pattern respectively. As a pre and post-operative care normal saline 0.5ml and Meloxicam 2mg/kg via subcutaneous route was given for 2 days. After 48h CLP/Sham surgery and 10 weeks CCL4/Olive oil mice were sacrificed to isolate EV from the plasma (n=4) from each groups.

EV from four groups of mice were isolated using the above mentioned method of differential ultracentrifugation. The EV  $1 \times 10^8$ /mouse (15) intravenously from respective groups were adoptively transferred via the tail vein. The schema of the experiment was as given below, and depicted in Figure 4A:

Group 1- Wild type received EV from wild type with control(olive oil) treatment of 10 weeks (n=5)

Group 2 - Wild type received EV from CCL4 (10 weeks) cirrhotic mice (n=5)

Group 3 - Wild type received EV from 48h post CLP septic mice (n=5)

Group 4 - Wild type received EV from 48h post sham surgery mice (n=5)

After 24h of adoptive transfer, the mice were sacrificed. The total leucocyte count, differential leucocyte counts, platelets, ALT, AST were measured in the whole blood. The liver infiltrating leucocytes, CD11b+, CD3+, CD19+ and F4/80+ cells were measured and analysed using multicolour flow cytometry. Histopathology of the liver and bone marrow of the recipient mice were also studied.

#### **Statistical Analysis:**

Statistical analyses were performed using Prism software v.7 (Graph Pad) and SPSS (IBM Analytics, USA). The data sets were first evaluated for normality of the data distribution. Statistically significant differences between samples were determined as appropriate using the Kruskal-Wallis test followed by post-hoc comparison using Scheffe method. Differences between categorical variables were assessed through the Fisher's exact test. Correlations were calculated using the Spearman's test. The univariate and multivariate analysis was also performed, the significant variables were subjected for cox-regression analysis. All statistical tests significance level was considered at  $p < 0.05$ . High dimensional analysis of flow cytometry data was performed through Barnes-Hut, t-distributed stochastic neighbour embedding (t-SNE) analysis using FCS express version 6.0 software (De novo software, USA).

## **RESULTS**

**Patient Characteristics:** Patients with cirrhosis, with and without sepsis were recruited as follows: Child-A, n=15; Child-B, n=16; Child-C, n=43; Child-C with sepsis, n=38. The demographic and the clinical profile of the

patients are tabulated in Table.1. Significant differences were present at baseline Child A, B and C patients. In Child C the one-month mortality was 48%.

#### **Circulating Extracellular Vesicle Signatures In Cirrhosis:**

We investigated EV released from immune cells in cirrhotic patients. The size and concentration of plasma EV are shown in Figure 1A. Absolute counts of monocyte, neutrophil and HSC-associated EV were significantly higher with increase in stage of severity (Figure 1B). However, no differences were found in EV associated with T or B cells and dendritic cells (Figure 1B). Additionally, ASGPRII+ EV, which are hepatocyte associated, were found to be increased in Child C than HC ( $p<0.025$ ) (Supplementary Figure 2A). EV associated with endothelial cells (CD31+), were also increased in Child C patients compared to controls ( $p<0.001$ ) (Supplementary Figure 2B). However, neutrophil cell population also significantly increased with Child stage (Child A versus C;  $p=0.022$ , Child B versus C;  $p=0.0152$ ). On the other hand, monocyte population linearly and significantly declined (Child A versus B;  $p=0.044$ , Child B versus C;  $p<0.0001$ , Child A versus C;  $p<0.0001$ ). The dendritic cells were higher in Child A compared to healthy controls ( $p<0.001$ ). The number of hematopoietic stem cells in circulation also progressively decreased with Child stage; Child A versus HC;  $p=0.003$ , Child A versus C;  $p<0.0001$ , Child B versus C;  $p<0.001$  (Supplementary Figure 1A and B). The lymphoid population, such as T cell subtypes (CD3+CD4+; CD3+ CD8+) and B cells were found to be significantly decreased in liver cirrhosis than HC ( $p<0.001$ ) but not among the various stages of cirrhosis (Supplementary Figure 1A and B).

Interestingly, on investigating mRNA levels inside EV from child C patients with and without sepsis, we found mRNA levels of IL-1b, Caspase3 to be significantly increased in the EV of patients with sepsis than without sepsis (Supplementary Figure 3). However, there were no significant change in the NLRP3, TNF-a, CXCR1, CCR3, BCL2 levels.

#### **Extracellular Vesicle Levels are Associated with Mortality in Sepsis in Cirrhosis Patients:**

We investigated the EV profile in Child C patients with no sepsis and with sepsis. The EV from monocytes, neutrophils and HSC were significantly elevated in Child C patients with sepsis than no sepsis ( $p<0.001$ ;  $p=0.017$ ;  $p=0.002$  respectively) (Figure 2A). The total leukocyte counts were also significantly high in sepsis patients than without sepsis ( $p=0.018$ ). Differential leukocyte count (DLC), neutrophils were significantly higher in patients with sepsis than no sepsis ( $78.5\pm 15.2$  vs  $64.2\pm 10.8$ ;  $p=0.038$ ). An additional analysis with TLC adjusted also showed elevated monocytes EV in sepsis than without sepsis Child C cirrhosis patients

( $p=0.028$ ) (Supplementary Table.1 ). However, the associated cell populations of neutrophils were high in Child C with sepsis than no sepsis ( $p=0.018$ ), monocytes, HSC and dendritic cells declined in Child C sepsis than no sepsis ( $p=0.0164$ ;  $p=0.008$ ;  $p=0.059$  respectively) (Supplementary Figure 1C). Univariate and multivariate analysis (Table 2) highlighted that monocyte as cells ( $p=0.045$ ; OR-586), monocyte associated EV ( $p<0.001$ ) were distinctly different in Child C with sepsis than no sepsis (Table 2). Circulating monocyte EV levels showed the highest AUROC (Area-0.76) ( $p<0.001$ ) and were best to predict survival in sepsis patients (Figure 2B). Based on the AUROC of monocyte EV, a cut-off value of 53 EV/ $\mu\text{l}$  or more showed 80% sensitivity and 73% specificity for survival. The Kaplan-Meier curve analysis elucidated a decrease in 1-month mortality in sepsis patients with monocyte EV  $<53$  EV/ $\mu\text{l}$  (log rank $<0.01$ ; Figure 2C) in Child C without sepsis, the mortality was 25%, whereas in Child C with Sepsis group, it was 44.7%. Hence, increased monocyte EV strongly correlate with sepsis and mortality in cirrhosis patients. Additionally, the leucocyte count ( $p=0.036$ ; OR-1.062) and neutrophil count ( $p=0.007$ ; OR-10.283) were also different in the septic cirrhotic patients.(Table 2).

#### **Circulating Extracellular Vesicles Communicate with Monocytes:**

Since the EV associated with monocytes in circulation were highest, and, also the monocyte population was significantly low and non-functional in patients of Child C with sepsis in comparison to without sepsis, we further investigated the role of EV in monocyte functions by co-culturing the healthy monocytes with EV isolated from Child C cirrhosis with sepsis and no sepsis for 24h (same as described previously)(9). First, we investigated whether EV are taken up by healthy monocytes. We observed that PKH67 (red) dye accumulated inside the monocytes, near the perinuclear area. (Figure 3A).

#### **Sepsis EV Induced Migration Arrest in Monocytes:**

EV direct the migration by synthesizing and releasing chemotactic signals. We performed the migration assay. We found EV from sepsis patients arrested the mobility of healthy monocytes whereas EV from without sepsis patients also showed slow mobility in comparison to controls or MCP-1, at 2h (Treatment with sepsis EV versus no sepsis EV  $p=0.002$  at 2h) at 4h ( $p<0.03$ )(Figure 3B). No differences were found at 6 and 12h (data not shown).

#### **Bioenergetics Capacity of Monocytes Post Sepsis EV treatment:**

Activation of immune cells is associated with enhanced energy demand. Therefore, we evaluated whether EV from two different groups induce oxidative phosphorylation as a more efficient and alternative mechanism for ATP generation. We measured resting oxygen consumption rate (OCR) and the mitochondrial respiratory profiles of monocytes after treatment with EV (Figure 3C). Rotenone-insensitive (i.e., residual cellular) OCR, reflecting oxygen consumption by non-mitochondrial sources, was similar between the groups (Figure 3C). Basal oxygen consumption rate was significantly reduced in cirrhotic with sepsis than no sepsis. Moreover, basal mitochondrial respiration was significantly lower in sepsis EV treated monocytes, than healthy EV treated cells ( $p=0.03$ ) (Figure 3C). OCR attributable to ATP production and proton leak was also comparable between the groups. Interestingly, we found non-mitochondrial respiration to be significantly induced by EV from Child C cirrhosis without sepsis than other cirrhosis groups ( $p<0.001$ ).

**Phagocytosis in Monocytes:** The functional capacity of healthy monocytes after EV incubation from patients with and without sepsis were measured. Interestingly, we found a significant increase in phagocytosis in monocytes induced by EV of Child C cirrhosis without sepsis compared with EV from cirrhosis with sepsis and EV from healthy controls ( $p=0.045;0.031$ ) (Figure 3D).

**EV Induced Gene and Cytokines Associated with Pro-inflammation:** qRT PCR was done for genes associated with apoptosis, inflammation and sterile inflammation and we found Casp3, IL-1b, NLRP3, IL-33 genes were significantly upregulated in monocytes treated with EV from sepsis patients (Figure 3F). Significant increase were seen in proteins levels of IL-1b ( $p<0.001$ ) and TNF-a ( $p<0.001$ ) in supernatants septic EV cultures than without sepsis EV. (Figure 3E).

#### **Adoptive transfer of Septic Extracellular Vesicles Induced Sepsis like Condition in Mice:**

EV were isolated from various groups of mice and adoptively transferred in wild type mice (as above, methods section) (Figure 4A). After 24h, the wild type mice were sacrificed. The biodistribution of EV was seen by PKH67 (red colour) (Supplementary Figure 5A-E) labelled EV. The blood count analysis showed a significant increase in platelet counts in sepsis EV recipient mice than control and no treatment recipient mice ( $p=0.043;0.001$ ). The leucocyte count was reduced in sepsis EV than cirrhotic EV recipients; and no treatment ( $p=0.030; 0.041$ ) (Figure 4B). However, no changes were observed in absolute counts of immune cells in blood (Figure 4B). Further, the intrahepatic immune cells were also investigated in all the groups.

Interestingly, we found CD11b+ cells in the liver significantly increased in sepsis EV recipients than cirrhotic EV and controls ( $p=0.033;0.023$ ) (Figure 4C). Also, the liver histology showed Kupffer cell hyperplasia in liver in septic EV group with lobular and portal inflammation in cirrhotic EV recipients (Figure 4D). Upon bone marrow evaluation we found increased neutrophils and hyperplasia in septic EV recipients and erythroid hyperplasia in cirrhotic EV and no significant changes were observed in controls (Figure 4E).

#### **DISCUSSION:**

The results of this study show for the first time, that plasma EV levels and specifically EV derived from monocytes, neutrophils and HSCs, progressively increase in patients with Child A to Child C, and furthermore, with development of sepsis. The monocyte EV levels were, in fact, able to predict the mortality in cirrhotic patients. EV were found to induce functional defects in the healthy monocytes which may be contributing to the development of sepsis in cirrhosis patients. Importantly, the results show, that the adoptive transfer of EV in wild type mice leads to the development of sepsis like conditions in mice and validates the seminal role of EV in precipitating sepsis in Child C cirrhosis patients.

Liver cirrhosis impairs synthesis of innate immunity proteins including pathogen recognition receptors, thereby, reducing the bactericidal capacity of phagocytic cells (16). Given the large functional reserve of the liver, lowered serum levels of these proteins are only evident in patients with advanced cirrhosis and ascites. This increases the susceptibility to bacterial infection and development of sepsis (17).

To understand the mediators of immune cell communication and immunodeficiency associated with cirrhosis, we studied the circulating immune cell population associated EV in different stages of cirrhosis. We also observed striking differences in their cell of origin during various stages of cirrhosis and sepsis.

Liver cirrhosis alters the number, subsets, distribution and functionality of circulating monocytes and neutrophils(18)(19). The expansion of the monocytes with limited phagocytic activity is observed regardless of the aetiology. In fact, ACLF patients manifest 'early' reduction in HLA-DR expression on monocytes with reduced ability to produce TNF- $\alpha$ , which may represent a physiological down-regulation of monocyte function and clearly shows monocyte defects but what propels this stimulation was largely unknown(20). However in our study also we observed EV associated with monocytes, neutrophils were progressively increasing which is reflective of cell of origin specific death or stress and it further increased in Sepsis and hence was able to

Accepted Article  
predict the mortality in cirrhosis patients. One of important finding of our study is that the EV concentration and levels could predict mortality in cirrhosis patients with sepsis. Child C patients with sepsis, having monocyte derived EV of >53 per  $\mu\text{l}$ , had a higher probability of death. This data needs to be validated in larger cohorts of cirrhosis patients. Study of EV gives us an opportunity to identify them as potential sepsis biomarkers.

T cell lymphopenia is common in cirrhosis and affects T helper and cytotoxic T cell functions(21).Although, in our study, we found alterations in the T and B cell subsets, but this did not attain significance, either in the cell populations or in associated EV.

Bone marrow is considered as a major site of haematopoiesis. We have previously shown that with increase in severity of cirrhosis, the loss of HSCs, with haematological and immunological dysfunctions occurs. This is also associated with reduced hepatic regeneration (22).In the current study, we observed thatCD34+ HSCs progressively increased, which could be reflective of excessive CD34+ cell death, indicating that the bone marrow reserve is being depleted (data not shown) in advanced cirrhosis and this is further compromised once sepsis develops.

Another important finding of our study was the seminal biological role of EV in development of sepsis in cirrhosis. Our data shows that EV communicate with monocytes and modulate their functions in cirrhotic patients. EV are known to participate in cell communication, immune regulation (23) and host response to microbial infections and inflammatory antigens. EV help in monocyte adhesion and their trans-endothelial migration (24). We found EV from cirrhosis patients with sepsis to induce mobility arrest in monocytes within 4h, however we observed slow migration even in cirrhosis patients as determined with the help of trans-well assays. These EV upregulated pro-inflammatory genes and higher IL-1 $\beta$  and TNF- $\alpha$  in supernatants of the culture. These data clearly indicate that EV contribute to the immune dysfunction and inadequate monocyte response during evolution of sepsis in cirrhosis patients.

The main limitation in our study was lack of details of the composition of EV cargoes in Child C patients with and without sepsis. Our experiments did show that the septic EV were able to induce sepsis like condition within 24h in a wild type mouse, which clearly indicating that they carry cargoes which are responsible for

sepsis. We also demonstrated that the mRNA levels of inflammatory genes were upregulated in EV of sepsis patients. Further investigations are needed to understand the mechanism by which EV induce a sepsis like condition. Another drawback is the lack of longitudinal follow-up of patients of cirrhosis before and after the development of sepsis to understand the dynamic changes in EV and their role in the development of sepsis. And another limitation was that all the Child C with sepsis patients enrolled were hospitalised, whereas the comparison group Child C without sepsis were from out-patient department.

Activation of immune cells is associated with enhanced energy demand. Therefore, we evaluated whether EV from two different groups induce oxidative phosphorylation as a more efficient and alternative mechanism for ATP generation. The sepsis EV reduced the basal metabolic capacity of the monocytes and immune cells. This data explains the potential of EV in modulating the immune responses in patients with cirrhosis and sepsis. Understanding how the EV from different immune cell types interact and regulate the host immunity, should result in the development of new therapeutic approaches.

Conceptually, our understanding of the natural history of cirrhosis has progressed over recent years, which describes patients with cirrhosis who progress from stable or decompensated cirrhosis to a rapid decline in liver function and extra-hepatic organ failure but still there are a few studies that examine immune cell phenotypes in different stages of the disease. Our study is the first which investigated comprehensively, the immune cells and associated EV in circulation from both innate and adaptive components.

Our study highlights several potential mechanisms that may explain the increased susceptibility to infections and the role of EV. Also, recently, it has been described that most cytokines/chemokines in septic mouse serum exist in two forms; the soluble free form and the insoluble exosome form. It has been shown that the exosomes from septic mice are immune-reactive and have the capability to enhance immune cells differentiation, promote cell proliferation and augment migration. Pre-administration of exosomes from septic mice not only suppresses cytokine production and alleviates tissue injury, but also prolongs the survival of the animals (25). Whereas, in our study also septic EV were able to induce the sepsis like conditions in wild type mice depicting its potential in development of sepsis.

In conclusion, our novel data demonstrates that extracellular vesicles manipulate monocyte function and help to understand the possible mechanism of development of sepsis in cirrhotic patients. Study of EV gives us an

opportunity to identify them as potential sepsis biomarkers and pave way to develop EV based therapeutic strategies.

## REFERENCES:

1. Asrani SK, Devarbhavi H, Eaton J, Kamath PS. Burden of liver diseases in the world. *J Hepatol*. 2019;70(1):151–71.
2. Nusrat S, Khan MS, Fazili J, Madhoun MF. Cirrhosis and its complications: Evidence based treatment. *World J Gastroenterol WJG* [Internet]. 2014 May 14 [cited 2020 Dec 17];20(18):5442–60. Available from: <https://www.ncbi.nlm.nih.gov/pmc/articles/PMC4017060/>
3. Malik R, Mookerjee RP, Jalan R. Infection and inflammation in liver failure: two sides of the same coin. *J Hepatol*. 2009 Sep;51(3):426–9.
4. Tilg H, Moschen AR, Kaneider NC. Pathways of liver injury in alcoholic liver disease. *J Hepatol*. 2011 Nov;55(5):1159–61.
5. Albillos A, Lario M, Álvarez-Mon M. Cirrhosis-associated immune dysfunction: distinctive features and clinical relevance. *J Hepatol*. 2014 Dec;61(6):1385–96.
6. Malhi H. Emerging role of extracellular vesicles in liver diseases. *Am J Physiol Gastrointest Liver Physiol*. 2019 Nov 1;317(5):G739–49.
7. Lemoine S, Thabut D, Housset C, Moreau R, Valla D, Boulanger CM, et al. The emerging roles of microvesicles in liver diseases. *Nat Rev Gastroenterol Hepatol*. 2014 Jun;11(6):350–61.
8. Lemoine S, Thabut D, Housset C, Moreau R, Valla D, Boulanger CM, et al. The emerging roles of microvesicles in liver diseases. *Nat Rev Gastroenterol Hepatol*. 2014 Jun;11(6):350–61.
9. Maji S, Matsuda A, Yan IK, Parasramka M, Patel T. Extracellular vesicles in liver diseases. *Am J Physiol Gastrointest Liver Physiol*. 2017 Mar 1;312(3):G194–200.
10. Sukriti S, Maras JS, Bihari C, Das S, Vyas AK, Sharma S, et al. Microvesicles in hepatic and peripheral vein can predict nonresponse to corticosteroid therapy in severe alcoholic hepatitis. *Aliment Pharmacol Ther*. 2018 Apr;47(8):1151–61.

- Accepted Article
11. Martin-Mateos R, Alvarez-Mon M, Albillos A. Dysfunctional Immune Response in Acute-on-Chronic Liver Failure: It Takes Two to Tango. *Front Immunol.* 2019;10:973.
  12. Gieseler F, Ender F. Extracellular Vesicles and Cell-Cell Communication: New Insights and New Therapeutic Strategies Not Only in Oncology. *Int J Mol Sci.* 2020 Jun 18;21(12).
  13. Riva A, Mehta G. Regulation of Monocyte-Macrophage Responses in Cirrhosis—Role of Innate Immune Programming and Checkpoint Receptors. *Front Immunol* [Internet]. 2019 Feb 5 [cited 2020 Jun 26];10. Available from: <https://www.ncbi.nlm.nih.gov/pmc/articles/PMC6370706/>
  14. Singer M, Deutschman CS, Seymour CW, Shankar-Hari M, Annane D, Bauer M, et al. The Third International Consensus Definitions for Sepsis and Septic Shock (Sepsis-3). *JAMA* [Internet]. 2016 Feb 23 [cited 2020 Dec 17];315(8):801–10. Available from: <https://www.ncbi.nlm.nih.gov/pmc/articles/PMC4968574/>
  15. Wiklander OPB, Nordin JZ, O’Loughlin A, Gustafsson Y, Corso G, Mäger I, et al. Extracellular vesicle in vivo biodistribution is determined by cell source, route of administration and targeting. *J Extracell Vesicles* [Internet]. 2015 Apr 20 [cited 2020 Dec 17]; Available from: <https://www.tandfonline.com/doi/abs/10.3402/jev.v4.26316>
  16. Albillos A, de la Hera A, González M, Moya J-L, Calleja J-L, Monserrat J, et al. Increased lipopolysaccharide binding protein in cirrhotic patients with marked immune and hemodynamic derangement. *Hepatol Baltim Md.* 2003 Jan;37(1):208–17.
  17. Bunchorntavakul C, Chamroonkul N, Chavalitdhamrong D. Bacterial infections in cirrhosis: A critical review and practical guidance. *World J Hepatol.* 2016 Feb 28;8(6):307–21.
  18. Vergis N, Khamri W, Beale K, Sadiq F, Aletrari MO, Moore C, et al. Defective monocyte oxidative burst predicts infection in alcoholic hepatitis and is associated with reduced expression of NADPH oxidase. *Gut.* 2017;66(3):519–29.

- Accepted Article
19. Korf H, du Plessis J, van Pelt J, De Groote S, Cassiman D, Verbeke L, et al. Inhibition of glutamine synthetase in monocytes from patients with acute-on-chronic liver failure resuscitates their antibacterial and inflammatory capacity. *Gut*. 2019;68(10):1872–83.
  20. Wasmuth HE, Kunz D, Yagmur E, Timmer-Stranghöner A, Vidacek D, Siewert E, et al. Patients with acute on chronic liver failure display “sepsis-like” immune paralysis. *J Hepatol*. 2005 Feb;42(2):195–201.
  21. Markwick LJJ, Riva A, Ryan JM, Cooksley H, Palma E, Tranah TH, et al. Blockade of PD1 and TIM3 restores innate and adaptive immunity in patients with acute alcoholic hepatitis. *Gastroenterology*. 2015 Mar;148(3):590-602.e10.
  22. Bihari C, Anand L, Rooge S, Kumar D, Saxena P, Shubham S, et al. Bone marrow stem cells and their niche components are adversely affected in advanced cirrhosis of the liver. *Hepatol Baltim Md*. 2016;64(4):1273–88.
  23. Mause SF, Weber C. Microparticles: protagonists of a novel communication network for intercellular information exchange. *Circ Res*. 2010 Oct 29;107(9):1047–57.
  24. Rautou P-E, Leroyer AS, Ramkhelawon B, Devue C, Duflaut D, Vion A-C, et al. Microparticles from human atherosclerotic plaques promote endothelial ICAM-1-dependent monocyte adhesion and transendothelial migration. *Circ Res*. 2011 Feb 4;108(3):335–43.
  25. Gao K, Jin J, Huang C, Li J, Luo H, Li L, et al. Exosomes Derived From Septic Mouse Serum Modulate Immune Responses via Exosome-Associated Cytokines. *Front Immunol [Internet]*. 2019 Jul 12 [cited 2020 Jun 26];10. Available from: <https://www.ncbi.nlm.nih.gov/pmc/articles/PMC6640201/>

**Table.1: Demographic and Clinical Profile of Liver Cirrhosis Patients.**

	Child A (n=15)	Child B (n=16)	Child C No Sepsis (n=43)	Child C Sepsis (n=38)	p-Value			
					Child A vs B	Child A vs C	Child B vs C	Child C No Sepsis vs Sepsis
Age (years)	40±7	49±8	45±8	48±10	-	-	-	-
Gender(M:F)	All Males	All Males	All Males	45;3	-	-	-	-
Hb (g/dl)	11.0±1.6	10.4±1.4	8.5±3.6	8.3±2.3	-	<b>0 .00</b>	<b>0 .00</b>	-
TLC ( 10 <sup>3</sup> cells/ml)	4.9±2.3	3.5±1.2	9.3±4.3	15.3±8.6	-	<b>0 .00</b>	<b>0 .00</b>	<b>0.032</b>
Neutrophils (%)	54±12	72±10	74.9±10.0	74.6±14.0	<b>0.022</b>	<b>0 .00</b>	<b>0.028</b>	-
Lymphocytes (%)	26±3	16±2.2	14.3±5.5	10.9±6.5	<b>0.001</b>	<b>0 .00</b>	<b>0.042</b>	<b>0.052</b>
Monocytes (%)	12±2	9±1.8	8.2±2.2	8.5±3.9	<b>0.012</b>	<b>0 .00</b>	-	-
Eosionophils(%)	6±4	3±1.5	3.3±2.7	2.0±2.7	<b>0.18</b>	<b>0 .00</b>	-	-
Platelets ( 10 <sup>3</sup> cells/ml)	145±23.4	122±32.1	110±22.1	95.8±66.7	-	<b>0 .00</b>	<b>0.058</b>	-
PT (sec)	16±12	18±6.5	19±4.5	20.7±7.4	-	-	-	-
INR	1.3±0.6	1.5±0.8	1.7±1.2	1.9±0.8	-	<b>0 .00</b>	-	-
Creatinine (mg/dl)	0.7±0.2	0.8±0.3	1.7±0.8	2.1±1.1	-	-	<b>0.032</b>	-
Total Bilirubin (mg/dl)	1.3±0.6	2.5±1.7	10.6±12.3	7.4±6.2	<b>0.001</b>	<b>0 .00</b>	<b>0 .00</b>	-
AST (IU/ml)	46.6±15.6	92.5±38.9	108.9±34.7	790±290	<b>0.025</b>	<b>0.01</b>	-	<b>0 .00</b>
ALT (IU/ml)	33.0±23.1	45±16.9	72.5±58.6	676.5±225	-	-	-	<b>0 .00</b>
Albumin (g/dl)	3.1±0.7	2.7±0.4	2.3±1.1	2.6±0.84	-	-	-	-
Ammonia (mg/dl)	150±20.1	153.6±28.6	164±64.9	172±44.9	-	-	-	<b>0 .00</b>
Mortality in 30 days %	-	-	12%	48%	-	<b>0 .00</b>	<b>0 .00</b>	<b>0 .021</b>

\* The symbol "-" depicts p-value greater than 0.05

### Legend

**Table 1:** Baseline characteristics of patients enrolled in study with different severity with child-pugh score.

The whole blood analysis, liver function test, kidney functions were different among the group of patients.

The mortality was high in Child C with sepsis than all the other groups.

**Table.2: Comprehensive Analysis of all the Clinical factors, percentage of cells and absolute numbers of Extracellular Vesicles among Child C patients with and without Sepsis.**

	Variables	Univariate						Multivariate			
		Child C No Sepsis	Child C Sepsis			95% CI for OR				95% CI for OR	
		Mean±SD	Mean±SD	p-Value	OR	Lower	Upper	p-Value	OR	Lower	Upper
Biochemical Factors	MELD	25.8±4.8	28.2±4.5	<b>0.038</b>	1.12	1.006	1.247	0.077	0.75	0.54	1.03
	Hb	10.5±1.9	8.3±2.1	<b>0.002</b>	0.454	0.277	0.744	-	-	-	-
	TLC	12.9±3.3	13.4±7.9	<b>0.018</b>	1.068	1.011	1.128	<b>0.038</b>	<b>1.126</b>	<b>1.007</b>	<b>1.26</b>
	Albumin	2.3±1.1	2.6±0.7	0.128	1.752	0.851	3.604	-	-	-	-
% of Cells by Flow Cytometry	Neutrophils	45.0±18.2	56.6±16.5	<b>0.018</b>	6.218	1.74	22.218	<b>0.077</b>	<b>1.052</b>	<b>0.995</b>	<b>1.112</b>
	Monocytes	1.5±0.8	1.08±0.8	<b>0.016</b>	0.586	0.348	0.988	<b>0.009</b>	<b>0.133</b>	<b>0.029</b>	<b>0.605</b>
	Dendritic Cells	3.3±0.5	2.85±1.7	0.059	0.671	0.44	1.022	-	-	-	-
	HSC	0.2±0.1	0.2±0.1	<b>0.008</b>	1.172	0.914	1.503	-	-	-	-
	CD4+ T cells	11.4±2.8	8.9±3.5	0.921	0.974	0.579	1.638	-	-	-	-
	CD8+ T cells	2.8±1.1	3.7±0.4	0.79	1.048	0.74	1.487	-	-	-	-
	B cells	6.5±3.2	6.1±4.2	0.932	0.98	0.609	1.575	-	-	-	-
Absolute numbers of Extracellular Vesicles	Neutrophils EV	52.1±13.1	137.1±12.8	<b>0.017</b>	5.11	1.335	19.567	-	-	-	-
	Monocytes EV	39±11.8	85.6±18.5	<b>0</b>	6.201	2.418	15.905	<b>0.018</b>	<b>1.047</b>	<b>1.008</b>	<b>1.087</b>
	Dendritic Cells EV	12.3±9.5	22.8±16.5	0.206	1.4	0.831	2.357	-	-	-	-
	HSC EV	78.5±32.2	110.2±56.8	<b>0.002</b>	8.583	2.165	34.03	-	-	-	-
	CD4+ T cells EV	85.4±25.6	125.9±55.8	0.273	0.408	0.082	2.028	-	-	-	-
	CD8+ T cells EV	172.±26.5	221.5±52.6	0.146	0.654	0.368	1.16	-	-	-	-
	B cells EV	106.4±32.8	116.2±89.6	0.631	1.175	0.61	2.264	-	-	-	-

**Legend:**

**Table 2:** The univariate and multivariate analysis of all the parameters investigated in the study among all the groups.

Accepted Article

## Figure Legends:

**Figure 1: Circulating Extracellular Vesicles Levels During Various Stages Of Liver Cirrhosis:** (A) The representative histogram shows the quality, size and concentration of plasma isolated EV from healthy, Child A, Child B and Child C cirrhosis using Nano sight NS300. The Y-axis is concentration (particles/ml) and X-axis is size in nm. The representative image captured from the video of live EV, showing the Brownian motion used for concentration and size of nanovesicle. (B) The scatter plots depicts the absolute counts of EV, originated from various innate and adaptive immune cells, as identified by the surface markers by flow cytometry. The threshold during acquisition of EV was set on Annexin V+ EV. The size was gated according to latex size beads in range between 0.22 $\mu$ m to 1 $\mu$ m. The Y-axis shows the absolute numbers in EV/ $\mu$ l. Monocytes EV CD14+ CD16-, Neutrophil EV CD11b+CD16+, Dendritic cell EV lin-CD11b+CD11c+, Hematopoietic stem cell EV CD45+CD34+, CD3+CD4+ T helper cells, CD3+CD8+ T cytotoxic cells, CD3-CD19+ B cells. Abbreviation: EV; Extracellular vesicle.

**Figure 2: Extracellular Vesicle Levels Are Associated With Mortality In Cirrhosis And Sepsis:** (A) The scatter box plots shows the immune cells associated EV in systemic circulation in patients of Child C cirrhosis with no sepsis compared to with sepsis. (B) The Univariate and multivariate analysis monocyte EV and AUROC (Area-0.76) ( $p < 0.001$ ) and were best to predict survival in sepsis patients. Based on the AUROC of monocyte EV, a cut-off value of 53 EV/ $\mu$ l or more showed 80% sensitivity and 73% specificity for survival. (C) The Kaplan-Meier curve analysis elucidated an increase in 1-month mortality in sepsis patients with monocyte EV  $< 53$  EV/ $\mu$ l (log rank  $< 0.01$  ( $p = 0.013$ )).

**Figure 3: Circulating Extracellular Vesicle From Cirrhosis And Sepsis Patients Communicate With Monocytes:** Plasma EV from healthy donor, Child C cirrhosis patients with no sepsis and with sepsis were co-cultured with healthy monocytes (1 cell: 100 EV) for 24h and then analysed the functional changes in monocytes. (A) The representative immunofluorescence image shows the uptake of EV by monocytes. Where EV were labelled with PKH67 (red) dye (plasma membrane dye) and the original magnification is 200x. (B) The bar graphs shows the migration of monocytes from upper chamber to lower in trans well assay after treatment with EV, the Y-axis shows the number of monocytes migrated in  $10^5$  and MCP-1 treatment was used as apposite control and plasma which is EV minus as negative control. (C) The graphs shows the oxygen consumption rate (OCR) and extracellular acidification rate of monocytes when treated with EV from various group of patients.

The line diagram shows changes in OCR, mitochondrial and non-mitochondrial respiration changes after various treatments. The bar graphs shows changes in monocytes basal oxygen consumption rate and spare reserve capacity. (D). The histograms shows the differences in phagocytic activity of monocytes when cultures with healthy EV, Child C without sepsis EV and Child C with sepsis. (E) The scatter plots shows the cytokine levels in pg/ml for IL-1b, TNF-a and IL-10 in the supernatants post 24h of EV monocytes culture. (F) The bar shows the quantitative reverse transcriptase PCR analysis various candidate genes induction in monocytes after treatment with EV from different study groups.

**Figure 4: Adoptive Transfer of Septic Extracellular Vesicles Induced Sepsis Like Condition in Wild-Type Mice:**

C57/BL6J mice were treated with EV from various groups for 24h and after infusion the observations were done(A). Panel (B) shows the observation in peripheral blood, the platelets counts, TLC and differential cell counts. (C) The liver infiltrating immune cells CD11b+, F4/80+, total CD3+ T cells and total CD19+ B cells and ASGPR+ hepatocytes. (D). The representative photomicrograph of liver is shown after adoptive transfer with septic EV, cirrhotic EV in comparison to no treatment. (E) The representative photomicrograph of Bone marrow evaluation after adoptive transfer with septic EV, cirrhotic EV in comparison to no treatment in wild type healthy mice.

**Supplementary Figure 1: Percentage Frequency of Immune Cells in Cirrhosis and Associated Sepsis:**

(A) The representative dimensional reduction plots (t-SNE) depicts the different populations of innate and adaptive immune cells in healthy controls, Child A, Child B and Child C. Color annotation; blue (CD3+ lymphocytes), red (CD11b+ CD16+ neutrophils), yellow (CD16- CD14+ monocytes), green (CD3- CD19+ B lymphocytes), maroon (CD11b+ CD11c+ dendritic cells) and purple(CD34+ CD45+ hematopoietic stem cells). (B) The scatterplots shows the immune landscape in the systemic circulation at various stages of liver cirrhosis (Child A>B<C) compared with healthy controls. (C) In the Child C group, patients with no sepsis and with sepsis were compared for various immune cells.

**Supplementary Figure 2: Circulating Extracellular Vesicles :**

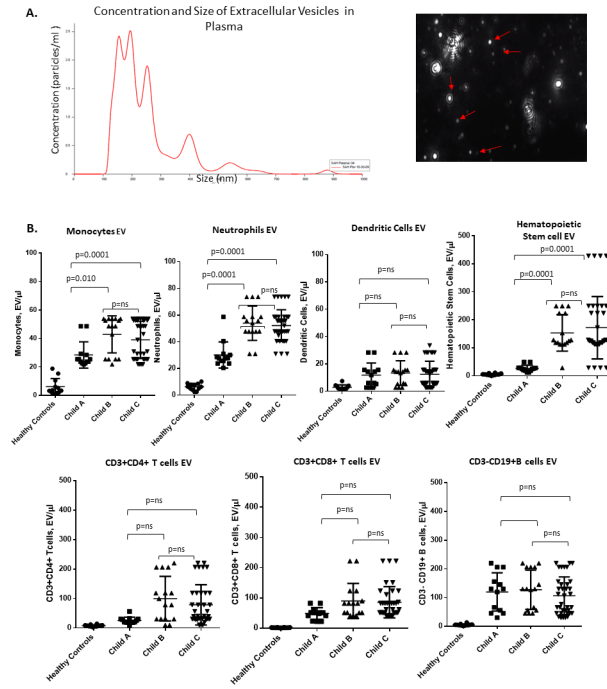
(A) The bar graphs shows the plasma levels of the EV associated with hepatocytes ASGPRII+ in Child A, B, C without sepsis and with sepsis compared with healthy controls. (B) endothelial cells (CD31+) associated EV.

**Supplementary Figure 3: mRNA Gene Expression In Extracellular Vesicles:** Upon investigating the mRNA levels in circulating EV from patients with Child C without sepsis and with sepsis, mRNA associated with inflammatory genes were differentially regulated. Black bar shows the healthy controls EV, grey shows the Child C without sepsis EV and dark shows the Child C with sepsis EV.

**Supplementary Figure 4: Gating Strategy:** (A) The gating strategy used for multicolour flowcytometry for the immune cells in human patients. (B) The gating strategy used for mouse immune cells stratification.

**Supplementary Figure 5: Biodistribution of Extracellular Vesicles in Various Organs :** (A) The PKH67 dye (red) was used to label EV before infusion and after 24h, the dye was located along EV in various organs such as Lung (B) Liver (C) Spleen (D) Kidney (E) Intestine.

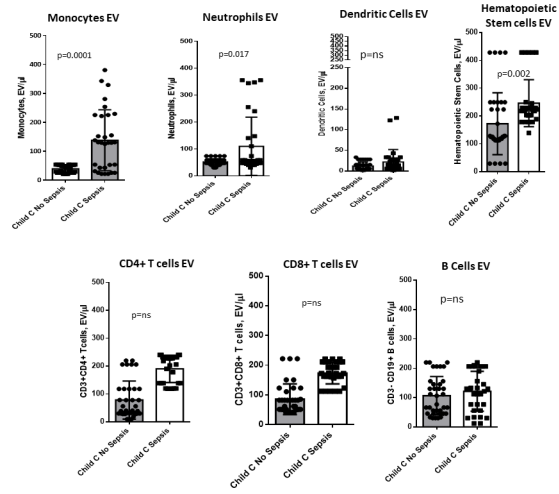
Figure.1



liv\_14875\_f1.tif

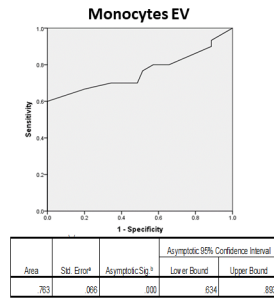
Figure.2

A.

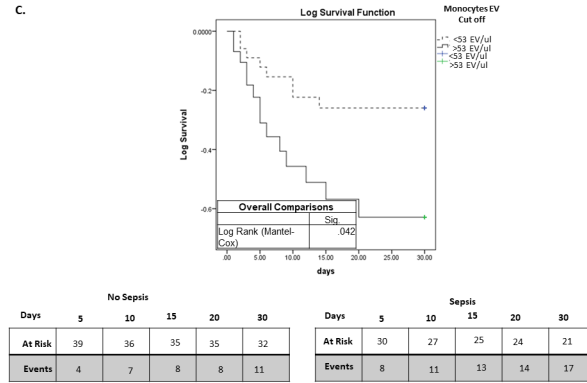


liv\_14875\_f2a.tif

B.

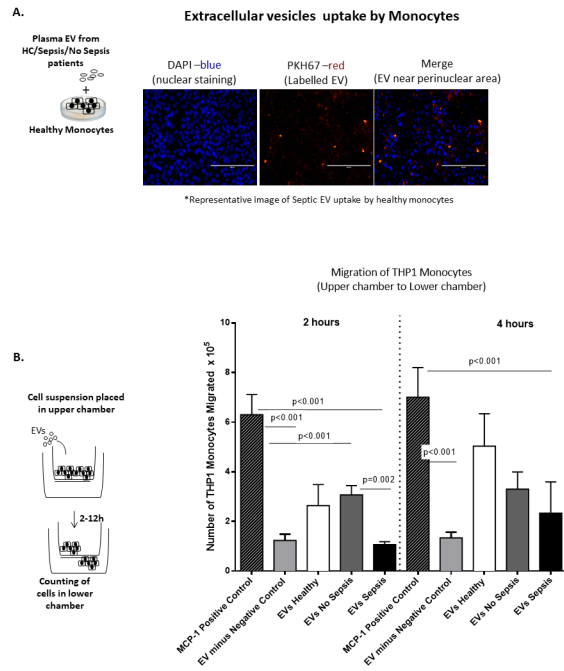


C.



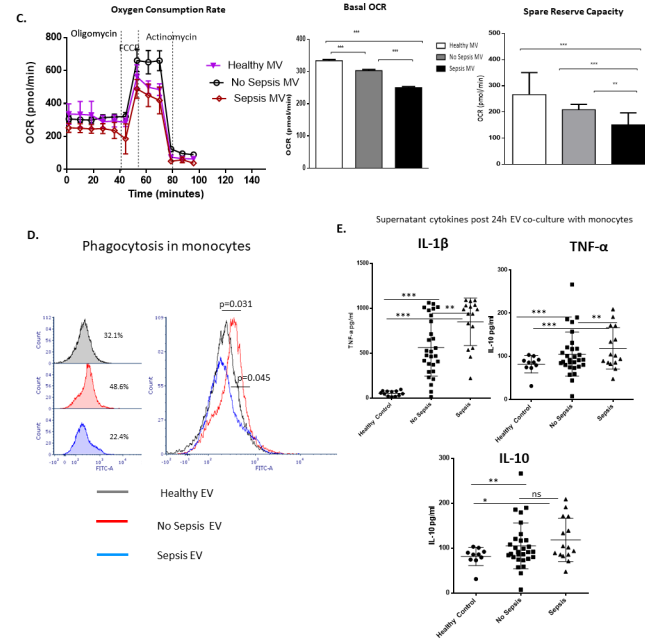
liv\_14875\_f2b-c.tif

Figure.3



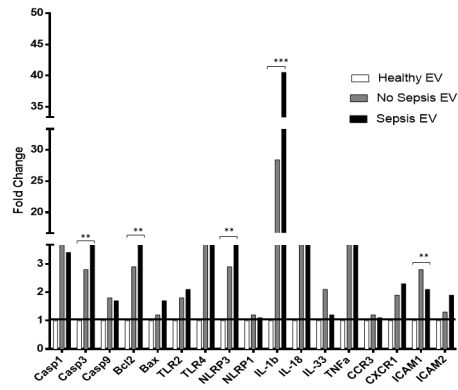
liv\_14875\_f3a-b.tif

Figure.3



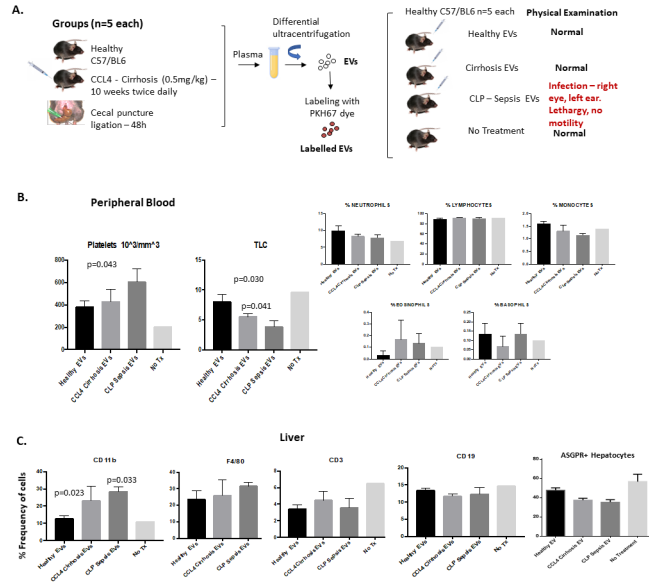
liv\_14875\_f3c-e.tif

F.

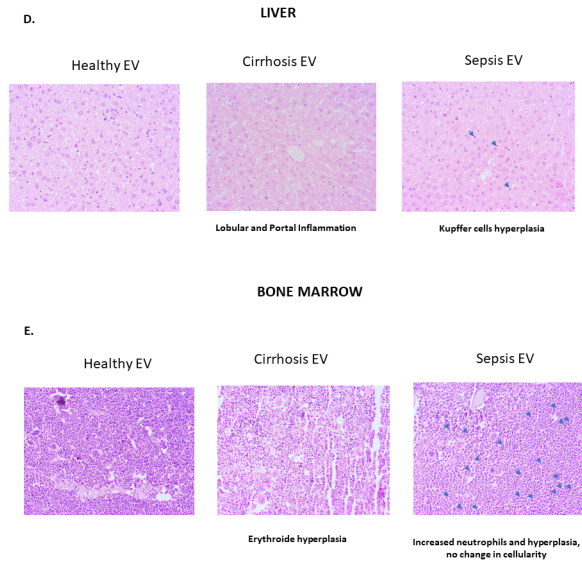


liv\_14875\_f3f.tif

Figure.4



liv\_14875\_f4a-c.tif



liv\_14875\_f4d-e.tif